IEEE Access
Multidisciplinary | Rapid Review | Open Access Journal

Received 8 December 2023, accepted 31 December 2023, date of publication 9 January 2024, date of current version 25 January 2024.

Digital Object Identifier 10.1109/ACCESS.2024.3351799

RESEARCH ARTICLE

UAV-Assisted Network Coded Cooperation by Using Height-Dependency Shaping Parameters in Nakagami-*m* Faded Channel

PANKAJ KUMAR[1] AND SUDHAN MAJHI[2], (Senior Member, IEEE)
[1]Department of Information and Communication Technology, Manipal Institute of Technology, Manipal Academy of Higher Education, Manipal 576104, India
[2]Department of Electrical Communication Engineering, Indian Institute of Science, Bengaluru 560012, India

Corresponding authors: Pankaj Kumar (pankaj.kumar@manipal.edu) and Sudhan Majhi (smajhi@iisc.ac.in)

ABSTRACT In this paper, we propose a height-dependency shaping parameter (m) and a height-dependency path-loss exponent for modelling small-scale Nakagami-m fading and a large-scale path-loss model for unmanned aerial vehicle (UAV)-assisted network coded cooperation (UA-NCC) system. The statistical parameters such as mean, variance, and probability density function (PDF) of the total noise component (TNC) are analyzed for the proposed system model to achieve the error free communication. We derive spectral efficiency, throughput, and a closed-form outage probability for the UA-NCC system by considering height-dependency shaping parameter (m) and the height-dependency path-loss exponent among ground-to-air (G2A) and air-to-ground (A2G) links, and Rayleigh channel distribution among ground users. The analytical result is validated with simulation results and compared it with the existing work (Rayleigh and Rician fading channel distribution). However, the better performance in the case of the proposed work comes over the existing state-of-the-art (Rayleigh and Rician fading distribution environment) after a UAV height of 10 m.

INDEX TERMS UAV, network coded cooperation, Nakagami-m channel, Rician and Rayleigh channel, outage probability, spectral efficiency, throughput.

I. INTRODUCTION

Due to exponential growing of smart devices in fifth generation and beyond (5GB), the demands of high reliability and higher spectral efficiency have been increased. The reliability can be improved either by using multiple input multiple output (MIMO) system [1] or by using cooperative communication (CC) [2]. The concept of network coding (NC) was proposed to achieve a better throughput [3]. The combination of NC and CC, called network coded cooperation (NCC), provides all the above benefits at one go, but most of the works is limited to stationary relay nodes [4], [5], [6], [7].

The use of NCC for unmanned aerial vehicle (UAV)-assisted communication, also known as UAV-assisted NCC (UA-NCC), is a perfect solution for 5GB in terms of energy efficiency, spectral efficiency and low latency communication. First UA-NCC was proposed in [8] to improve the diversity and throughput of the system over disaster/post-catastrophe scenarios. The authors analyzed performance of UA-NCC [9], [10] over an air-to-ground (A2G) channel model based on Rayleigh fading, Rician fading and the probability of occurrence of a line-of-sight (LoS) model. However, the probability-based channel model considered two extreme cases for modelling A2G links, i.e., Rayleigh or Rician fading, whereas in practice, these A2G links take any general fading distribution that lies between the Rayleigh and Rician channel models depending on the UAV height. In such scenarios, Nakagami-m fading channel model proves to be a more generalized channel model, which covers all the possible fading for ground-to-air (G2A) and A2G links depending on the values of m.

The associate editor coordinating the review of this manuscript and approving it for publication was Halil Ersin Soken.

The authors evaluated secrecy outage probability [11] using a Nakagami-m fading channel model for a fixed value of m. Some of the existing literature analyzed the performance of UAV-based CC [12], [13], [14], [15], [16], [17] by considering Nakagami-m fading channel model, where the shaping parameter is fixed and does not change with UAV height. The authors considered simple UAV [18] as an aerial base station for serving the ground internet of things (IoT) devices by considering Nakagami-m fading channel model, where the shaping parameters (m) varies with UAV height. The UAV-assisted downlink communication have been carried out [19], [20], [21], [22], [23], [24], and [25] for improving the reliability for ground users. However, these work does not consider NCC, hence diversity and high throughput can not be achieved.

During the literature survey we also found that most of the works are considered Drone/UAV as an aerial relay or base station for A2G communication. However, during developing the mathematical framework the authors consider either down link communication or Up link communication at a given communication cycle. They did not consider both uplink and downlink communications for the given scenario. For the same the authors consider height-independent Rayleigh, Rician, and Nakagami-m fading distributions for A2G links. Apart from that they also do not consider the network coding at UAV over the signal received during uplink communication cycle.

To the best of our knowledge, few literatures consider both uplink and downlink along with NC at UAV for the multi-user scenario [8], [9], [10]. The authors developed the framework for the UA-NCC system using Rayleigh, Rician, and combination of both (Rayleigh and Rician) channel distributions for A2G links for analysis purposes. However, they do not include all the channels (that lie between Rayleigh and Rician) variation with UAV height.

The existing literatures [8], [9], and [10] also did not address the analytical framework for the UA-NCC system while incorporating a height-dependent shaping parameter for modeling the Nakagami-m fading channel. The one solution for incorporating all the channel variation gain is Nakagami-m fading. It is more generalized fading where the channel gain can be changed with the height of UAV positions. Taking into account the fact that in practical scenarios, the variation in the channel parameters may change with the movement of an UAV. This leads to motivating us to propose the height-dependency m shaping parameter for modelling G2A and A2G links along with the height-dependency path-loss exponent for the UA-NCC system. Therefore, in this paper, we propose the height-dependency m factor for modelling G2A and A2G links along with the height-dependency path-loss exponent. The main contributions of this paper can be summarized as follows

- Height-dependency shaping parameter (m) is proposed for modelling the Nakagami-m fading channel model for G2A and A2G links.
- The height-dependency path-loss exponent is proposed for evaluating the large-scale attenuation.
- Spectral efficiency and throughput for the UA-NCC system are analyzed by considering the above system parameters.
- Closed-form outage probability for the UA-NCC system is derived by considering the above system parameters.
- The expressions for the total noise component (TNC) and its statistical analysis such as mean, variance, and probability density function (PDF) are analyzed to obtain the error free communication.

II. RELATED WORK

Authors in [8] discussed UA-NCC system in a Rayleigh fading environment. They derived a closed-form expression of an outage probability using amplify-and-forward (AF) at the UAV, a fixed path-loss exponent for large-scale fading and maximal ratio combining (MRC) at the destination node are adopted. The main problem associated with [8] is the assumption of fixed channel model between the source-UAV link and the UAV-destination link that does not change with UAV height, therefore affecting the actual performance of the UA-NCC system. The optimal placement of a UAV for a pair of ground users is discussed in [26]. The authors used height-independent shaping parameter for the Nakagami-m fading channel model and a height-dependent path-loss exponent to model the large-scale attenuation in deriving outage probability and bit error rate (BER). Due to the height-independent nature of shaping parameter [26], the actual performance in practical scenarios may be affected. The analytical closed-form expression of an outage probability is derived in [27] for the UA-NCC system using the Rician fading and a height-independent path-loss exponent for modelling large-scale attenuation. The destination node uses selection combining (SC) for the direct signal and the signal coming via the UAV, while the UAV use decode-and-forward (DF) relaying for decoding purposes. The height-independent Rician factor does not provide the actual characterization of A2G links [27], therefore the performance deviates from the true one in real-world scenarios. The analysis of the UA-NCC system is considered [9] in a probabilistic channel model where A2G links are assumed either Rayleigh or Rician based on the probability of occurrence of LoS. The authors considered the height-dependent path-loss exponent for measuring large-scale fading and analyzed the performance by using AF at UAV and MRC at the destination node. However, in a UAV-assisted network, the channel gain changes with the UAV height, while in [9] the authors considered only two extreme fading channels for modelling the A2G links. The closed-form expression of an outage probability [28] for the UA-NCC system is also derived by using Rayleigh as a small-scale fading and a fixed path-loss exponent for large-scale fading. The relaying scheme used at UAV is AF and SC is used at destination nodes for the purpose of analysis. However, in [28], the height-dependent parameters is not considered for modelling small-scale as well as large-scale

fading, which further affects the true performance of the network. Simulation-based outage analysis [29] is performed using AF at the UAV and MRC at the destination node in a probabilistic channel model. However, closed-form outage probability is not considered for the performance metric and the variations of fading that depend on UAV heights is also not considered in [29]. The performance of an intelligent reflecting surface (IRS)-assisted dual-hop UAV is analyzed in [30] using height-independent Rician fading for A2G links. However, the authors do not consider NCC and Rician factors as a function of UAV height for modelling the channel that affects the true performance of the network. The UAV-assisted IRS is considered in [31], [32], and [33], and evaluates the network performance in terms of outage probability, BER, and sum-rate by considering height-independent Rician fading, while in practice the Rician factor changes with UAV height. The performance metrics such as outage probability and rate for UAV-assisted CC are analyzed in [34] and [35] by considering the hybrid channel (Rayleigh-Nakagami-m) model, where the value of m is fixed with respect of UAV heights that restrict the actual performance. The authors discussed about UAV-assisted device-to-device (D2D) cooperative communication [36], where A2G links are assigned based on the probability of occurrence of LoS and height-independent path-loss exponent is used for large-scale path-loss model. The authors derive the closed-form outage probability expression [36] for the above model using AF at UAV and SC at the destination node. The absence of the height-dependent channel distribution parameters in [36] restricts the ability to accurately assess performance metrics at the destination node. The authors derived the closed-form expression of outage probability for UAV-assisted communication by considering an interference scenario [37]. However, the derivation does not include the effect of height on Nakagami-m fading distribution along with the NC at the UAV node. The authors in [38] discussed ground-to-UAV, UAV-to-UAV, and UAV-to-ground communication without considering NC at UAV. The outage probability expression is derived here by considering height independent Nakagami-m fading channel.

A. DIFFERENT ASPECTS OF UA-NCC SYSTEM

This sub-section discusses the various aspects of UAV assisted network coded cooperation. The discussion unfolds as follows:

1) NEED OF THE PROPOSAL

UAV-assisted network-coded cooperation (UA-NCC) leverages the fusion of UAV technology and NC to bolster wireless network communication. Although current research often assumes a fixed channel gain for A2G links, disregarding the dynamic channel gain with UAV altitude. This oversight directly impacts the UA-NCC system's performance, subsequently affecting the network's reliability. Therefore, we propose a height-dependent Nakagami-m shaping parameter to address the channel gain fluctuations with UAV altitude, ultimately improving the network's reliability.

2) CHALLENGES INVOLVED

Creating advanced hardware circuitry and streamlined algorithms to adapt NC in reaction to altitude-induced channel variations represents a significant challenge. Conducting real-world experiments to validate the effectiveness of height-dependent channel gain models in UA-NCC system is challenging. Acquiring accurate empirical data across various altitudes and environmental conditions is resource-intensive and complex.

3) ALREADY EXIST SOLUTION

There are ongoing developments exploring the integration of UAVs with NC techniques to enhance communication systems for fixed channel environments. While comprehensive, fully implemented solutions might still be evolving. Academia and research institutions have been working on prototypes that demonstrate the feasibility of using UAVs for NCC for fixed channel environments. These prototypes often focus on specific aspects like enhancing connectivity, optimizing data transmission, or improving network resilience.

4) LIMITATIONS AND DRAWBACKS

UAVs have limitations regarding the amount of equipment they can carry. Additionally, the range of drones is limited by battery life and regulations, affecting the coverage area they can provide. Operating UAVs in certain areas may be restricted due to aviation regulations or safety concerns, limiting their deployment in some regions or scenarios. Coordinating multiple drones for efficient NC tasks requires intricate planning and control, which can increase operational complexity and potential errors. The expenses associated with acquiring, operating, and maintaining UAVs for NCC can be substantial, impacting the feasibility of such systems.

The paper is structured as follows: In Section III, we delve into the system model utilized within this study. This section provides an intricate exploration of the mathematical framework for the UA-NCC system, elucidating the statistical parameters of the TNC. Various performance metrics (such as spectral efficiency, outage probability, throughput) are detailed in Section IV. Section V delves into the discussion of results and analysis. Finally, Section VI encapsulates the concluding remarks and discussions.

III. SYSTEM MODEL

Fig. 1 (a), shows the generalized scenario of the proposed system model. The key application of UA-NCC system is a disaster management scenario where the base station is not functional. In such scenarios, one can improve the reliability of the UA-NCC system by increasing the vertical position of the UAV, which improves the channel gain between the UAV and the end users. The scenario shown in Fig. 1 (a) consists of N number of transmitter (t_i)-receiver (r_i) pairs assisted by UAV, a relay node. Distance among UAV and the ground

TABLE 1. Summary of notations.

Symbol	Definition
N	Number of transmitter-receiver (t_i-r_i) pairs
U	Relay node
x_i	Signal transmitted by node i
d_{ij}	Distance between nodes i and j
$\hbar_{ij}$	Channel coefficient between nodes i and j
ξ_i	Additive white Gaussian noise (AWGN) at i^{th} node
σ_i^2	AWGN variation at the i^{th} node
$\mathbb{P}_i$	Power transmitted by i^{th} node
$\mathcal{Z}_{ij}$	Signal received at j^{th} node when i^{th} node transmits
$\sigma_{\mathbb{R}_i}^2$	TNC variation at the i^{th} node
Υ_{ij}	Signal-to-noise ratio (SNR) between i^{th} and j^{th} node
α	Path-loss exponent
j_1, j_2	Environmental parameters
m	Nakagami shaping parameter
h_D	UAV height
λ	Rate parameter for Gamma distribution

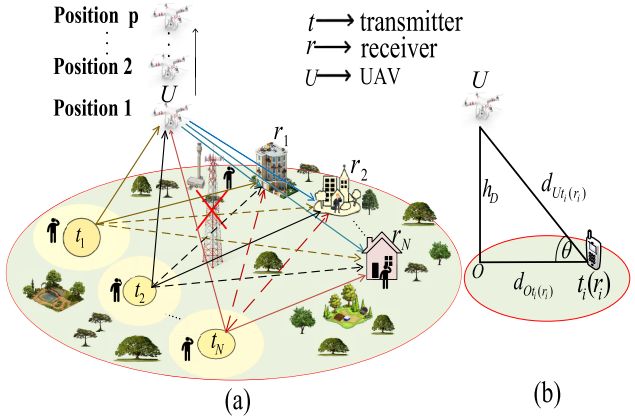

FIGURE 1. (a) Shows the generalized scenario for UA-NCC system [9], where t_i, $i \in \{1, 2, \ldots, N\}$ and r_i are the ith transmitter and receiver, respectively. U denotes relay node, and (b) shows the vertical position of UAV for a given horizontal configuration of ground users.

users can be calculated with the help of Fig. 1 (b), where d_{Ut_i}, d_{Ur_i}, d_{Ot_i}, d_{Or_i}, and h_D denote the distance between UAV and t_i/r_i, distance between vertical projection of U on the ground plane (O) and t_i/r_i, and UAV vertical height, respectively. The transmission-reception scheme is based on time division multiple access (TDMA) technique. In the ith time-slot, t_i transmits its data ($x_i, , i \in \{1, 2, \ldots, N\}$) to the desired r_i which is received by U and overheard by other r_j, where $j \in \{1, 2, \ldots, N\}, j \neq i$. The U performs DF relaying over the received data in the previous N time-slots and performs NC over the combined data and broadcasts it to the r_i in the $(N+1)$th time-slot. The 2nd copy of the desired data (x_i) can be extracted at r_i by using the data[1] (x_j) coming from the t_j and U nodes. SC is used for combining the two copy at the desired receiving (r_i) node. The channel between t_i (or r_i) and U changes significantly, therefore, these links are modelled by using Nakagami-m fading channel model with shaping parameter m that depends on height of U and environmental parameters, and parameters as defined in [18]

$$m = j_1 e^{j_2 \theta}, \tag{1}$$

where θ=tan$^{-1}\left(\frac{h_D}{d_{Ot_i(r_i)}}\right)$, j_1, and j_2 denote the environmental parameters. The minimum possible value of m is j_1 when θ=0 or UAV is positioned at the ground plane. Therefore for covering the Rayleigh fading ($m = 1$) scenario, we assume j_1=1. Furthermore, at $h_D = d_{Ot_i(r_i)}\tan\left(\frac{1}{j_2}\log_2\frac{(K+1)^2}{(2K+1)}\right)$ the Nakagami-m fading channel model is approximated to Rician distribution with rician factor K. The maximum value of m is achieved when θ becomes $\frac{\pi}{2}$ or UAV is positioned at very high altitude, i.e., $j_2 = \frac{2}{\pi}\log_2(m_{\max})$. In the proposed network, we also consider h_D dependent path-loss exponent [39] for modelling large-scale attenuation which is defined as

$$\alpha = (\alpha_L - \alpha_{NL})\chi_L + \alpha_{NL}, \tag{2}$$

where α_L and α_{NL} are path-loss exponents corresponding to χ_L and χ_{NL} (probability of occurrence of non LoS (NLoS)), respectively. In (2), χ_L corresponds to probability of occurrence of LoS and can be given as [8]

$$\chi_L = \frac{1}{1 + j_1 e^{j_1 j_2} e^{-j_2\theta}}. \tag{3}$$

The following assumptions that we consider during the analytical frame work of the UA-NCC system given as [8]

- Energy related issues associated with U are not considered here. All the nodes are assumed to be operated in half-duplex mode.
- Only receiver nodes has the complete channel state information (CSI).
- Packet size is the same for all nodes.
- The coherence time is long enough to complete a packet transmission. However, channel may change independently between two consecutive communication cycle.[2]
- The altitude and antenna height of t_i, r_i, and U are neglected in this study.

A. MATHEMATICAL FRAMEWORK FOR UA-NCC SYSTEM

Transmission-reception scheme for N t_i-r_i pairs is discussed in this subsection. In the proposed mathematical framework, Nakagami-m fading is assumed among G2A and A2G links and Rayleigh fading among ground nodes. Let us also consider t_i-r_i as a pair of interest. Signal received at r_i, r_j, and U can be written as

$$\mathcal{Z}_{t_i r_i}^{\mathrm{R}} = \sqrt{\mathbb{P}_{t_i} d_{t_i r_i}^{-\alpha}}\,\hbar_{t_i r_i}^{\mathrm{R}} x_i + \xi_{r_i}, \tag{4}$$

$$\mathcal{Z}_{t_i r_j}^{\mathrm{R}} = \sqrt{\mathbb{P}_{t_i} d_{t_i r_j}^{-\alpha}}\,\hbar_{t_i r_j}^{\mathrm{R}} x_i + \xi_{r_j}, \tag{5}$$

and

$$\mathcal{Z}_{t_i U}^{\mathrm{N}} = \sqrt{\mathbb{P}_{t_i} d_{t_i U}^{-\alpha}}\,\hbar_{t_i U}^{\mathrm{N}} x_i + \xi_U, \tag{6}$$

[1] It is not treated as interference at node r_i for the UA-NCC system because it is required during the extraction of the 2nd copy of the desired signal (x_i).

[2] One communication cycle consists of $N+1$ time-slots, the first N of which are associated with t_i and the last $(N+1)$th with U.

where R, N, $\mathcal{Z}_{ab}$, d_{ab}, $\mathbb{P}_a$, and x_a denote Rayleigh channel, Nakagami channel, the signal received at b from a, distance between nodes a and b, transmitted power and transmitted signal by node a, respectively. Symbol α denotes path-loss exponent, ξ_b denotes additive white Gaussian noise (AWGN). Here $\hbar_{ab}$ denotes channel coefficient between nodes a and b. U decodes (full decoding of x_i) the N signals, combine them, and forwards it to r_i node using DF relaying scheme. Received signal in $(N+1)$th time-slot at node r_i, can be written as

$$\mathcal{Z}^{\mathrm{N}}_{Ur_i} = \sqrt{\mathbb{P}_U d^{-\alpha}_{Ur_i}} \left[\sum_{i=1}^{N} x_i\right] \hbar^{\mathrm{N}}_{Ur_i} + \xi_{r_i}. \tag{7}$$

Without loss of generality, node r_i is considered for showing the extraction process of the 2nd copy of required data and appearance of residual term. After few simplifications by using (5) in (7), 2nd copy ($\hat{\mathcal{Z}}_{Ur_i}$) of required data at r_i can be expressed as

$$\hat{\mathcal{Z}}^{\mathrm{R,\,N}}_{Ur_i} = \underbrace{\sqrt{\mathbb{P}_U d^{-\alpha}_{Ur_i}} \hbar^{\mathrm{N}}_{Ur_i} x_i}_{\text{1st term}} + \underbrace{\xi_{r_i} - \sum_{j=1, j\neq i}^{N} \frac{\sqrt{\mathcal{P}_U d^{-\alpha}_{Ur_i}} \hbar^{\mathrm{N}}_{Ur_i}}{\sqrt{\mathcal{P}_{t_j} d^{-\alpha}_{t_j r_i}} \hbar^{\mathrm{R}}_{t_j r_i}} \xi_{r_j}}_{\text{2nd term}}. \tag{8}$$

In the above equation, the 1st term represents the desired part of the transmitted signal, while the 2nd term denotes the residual part comes due to the extraction of the desired signal, which is known as TNC. The occurrence of TNC in (8) is due to the extraction process of 2nd copy of required data. To extract the 2nd copy $\mathcal{Z}_{t_i U r_i}$ from the sum signal $(\mathcal{Z}_{t_i U r_i} + \sum_{j=1, j\neq i}^{N} \mathcal{Z}_{t_j U r_i})$ at r_i, the signal $\sum_{j=1, j\neq i}^{N} \mathcal{Z}_{t_j r_i}$ is subtracted from the sum signal $(\mathcal{Z}_{t_i U r_i} + \sum_{j=1, j\neq i}^{N} \mathcal{Z}_{t_j U r_i})$. This process results in residual term $\sum_{j=1, j\neq i}^{N} (\mathcal{Z}_{t_j U r_i} - \mathcal{Z}_{t_j r_i})$ due to asymmetric channel characteristics between paths t_j-r_i and t_j-U-r_i. Therefore, the final expression of the 2nd copy of x_i reaching at r_i via U is written as

$$\hat{\mathcal{Z}}^{\mathrm{R,N}}_{Ur_i} = \sqrt{\mathbb{P}_U d^{-\alpha}_{Ur_i}} \hbar^{\mathrm{N}}_{Ur_i} x_i + \mathbb{R}^{\mathrm{R,\,N}}_i, \tag{9}$$

where $\mathbb{R}_i$ denotes TNC (combined effect of AWGN and digital network coding (DNC) noise) at r_i, and given as

$$\mathbb{R}^{\mathrm{R,\,N}}_i = \xi_{r_i} - \underbrace{\sum_{j=1, j\neq i}^{N} \left(\frac{\sqrt{\mathbb{P}_U d^{-\alpha}_{Ur_i}} \hbar^{\mathrm{N}}_{Ur_i}}{\sqrt{\mathbb{P}_{t_j} d^{-\alpha}_{t_j r_i}} \hbar^{\mathrm{R}}_{t_j r_i}} \right) \xi_{r_j}}_{\text{DNC-noise}}. \tag{10}$$

The cumulative effect of TNC for UA-NCC system can be find by taking the average of (10) and given as

$$\mathbb{R}^{\mathrm{R,\,N}}_{\mathrm{system}} = \frac{\sum_{i=1}^{N} \mathbb{R}^{\mathrm{R,\,N}}_i}{N}. \tag{11}$$

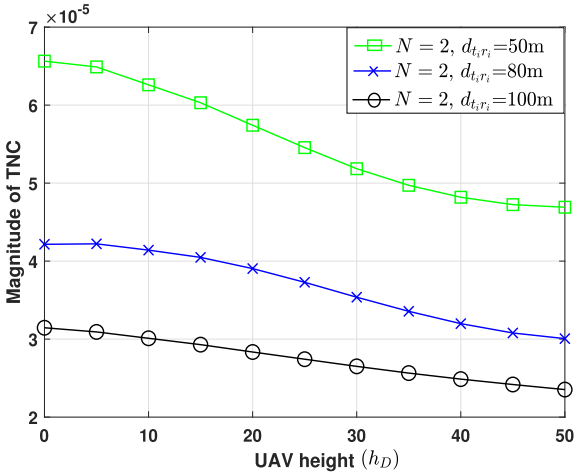

FIGURE 2. TNC magnitude with UAV height (meter) for N=2 t_i-r_i pairs.

Fig. 2 shows the variation of magnitude of TNC with UAV height for different configuration of t_i-r_i pairs. It may be noted here that the strength of TNC is greater when the t_i-r_i pairs are configured in such a way that the distance between them is less. The strength of TNC decreases with increase in the UAV height for all the configuration of t_i-r_i pair. This is happened because with an increase in UAV height, the value of m increases as a result (10) the strength of TNC decreases.

B. STATISTICAL PARAMETERS OF TNC

The statistical parameters of the TNC are mean, variance, and PDF, which will be derive in this subsection. By knowing these parameters of TNC, one can easily decode the transmitted signal from the received signal at the desired destination node.

1) MEAN

Because the background noise at nodes r_i and r_j is statistically independent and has a zero mean $\left(\mathrm{E}[\xi_{r_i}] = \mathrm{E}[\xi_{r_j}] = 0\right)$, therefore, the mean of (10) for a given UAV height is zero $\left(\mathrm{E}\left[\mathbb{R}^{\mathrm{Ray,\,Nak}}_i\right] = 0\right)$, where E [.] denotes the expectation operator.

2) VARIANCE

The variance of TNC at the desired node r_i is calculated by taking the variance on both sides of (10) and defining as

$$var\left[\mathbb{R}^{\mathrm{R,\,N}}_i\right] = var\left[\underbrace{\xi_{r_i} - \sum_{j=1, j\neq i}^{N} \left(\frac{\sqrt{\mathbb{P}_U d^{-\alpha}_{Ur_i}} \hbar^{\mathrm{N}}_{Ur_i}}{\sqrt{\mathbb{P}_{t_j} d^{-\alpha}_{t_j r_i}} \hbar^{\mathrm{R}}_{t_j r_i}} \right) \xi_{r_j}}_{\text{DNC-noise}}\right], \tag{12}$$

where **var** denotes variance of TNC. Taking statistical independence of the background noise ξ_i and ξ_j, variance of

$\mathbb{R}_i^{\mathrm{R,N}}$ is denoted by $\sigma^2_{\mathbb{R}_i^{\mathrm{R,N}}}$ and given as

$$\sigma^2_{\mathbb{R}_i^{\mathrm{R,N}}} = var\left[\xi_{r_i}\right] + var\left[\underbrace{\sum_{j=1,j\neq i}^{N}\left(\frac{\sqrt{\mathbb{P}_U d_{Ur_i}^{-\alpha}}\hbar^{\mathrm{N}}_{Ur_i}}{\sqrt{\mathbb{P}_{t_j} d_{t_jr_i}^{-\alpha}}\hbar^{\mathrm{R}}_{t_jr_i}}\right)\xi_{r_j}}_{\text{DNC-noise}}\right]. \tag{13}$$

Using the variance property and the assumption that $\hbar^{\mathrm{R}}_{t_jr_i}$ and $\hbar^{\mathrm{N}}_{t_jr_i}$ are constant over the course of a packet duration, the aforementioned equation can be expressed as

$$\sigma^2_{\mathbb{R}_i^{\mathrm{R,N}}} = var\left[\xi_{r_i}\right] + \sum_{j=1,j\neq i}^{N}\left(\frac{\mathbb{P}_U d_{Ur_i}^{-\alpha}|\hbar^{\mathrm{N}}_{Ur_i}|^2}{\mathbb{P}_{t_j} d_{t_jr_i}^{-\alpha}|\hbar^{\mathrm{R}}_{t_jr_i}|^2}\right) var\left[\xi_{r_j}\right]. \tag{14}$$

The average noise power at nodes r_i and r_j is $var\left[\xi_{r_i}\right]=\sigma^2_{r_i}$ and $var\left[\xi_{r_j}\right]=\sigma^2_{r_j}$. Therefore, the variance of TNC is given as

$$\sigma^2_{\mathbb{R}_i^{\mathrm{R,N}}} = \sigma^2_{r_i} + \sum_{j=1,j\neq i}^{N}\left(\frac{\mathbb{P}_U d_{Ur_i}^{-\alpha}|\hbar^{\mathrm{N}}_{Ur_i}|^2}{\mathbb{P}_{t_j} d_{t_jr_i}^{-\alpha}|\hbar^{\mathrm{R}}_{t_jr_i}|^2}\right)\sigma^2_{r_j}. \tag{15}$$

From (15), it is to be noted that the variance of TNC at r_i, increases with the number of t_i nodes. The cumulative effect of variance for the UA-NCC system can be found by taking the average of (15) and given as

$$\sigma^2_{\mathbb{R}^{\mathrm{R,N}}} = \frac{\sum_{i=1}^{N}\sigma^2_{\mathbb{R}_i^{\mathrm{R,N}}}}{N}. \tag{16}$$

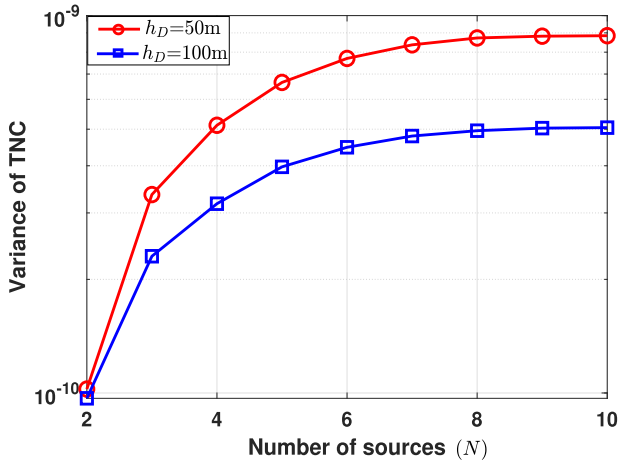

FIGURE 3. Varince of TNC with number of sources for different UAV heights.

Fig. 3 indicates the variance of the TNC with the number of sources for different UAV height. Here, it may be noted that the variance of TNC increases with the number of sources, the same is mentioned in (15). Fig. 3 indicates that the variance of TNC at h_D=50m is greater as compared to that of h_D=100m. This is because the path-loss exponent decreases with h_D, which may impact the large-scale fading.

3) PDF OF TNC

In this subsection, the PDF of TNC is derived by considering two t_i-r_i pairs. During the derivation, we assume that the channel coefficients will not change during the transmission of one packet duration or in one communication cycle. Using (10) for two t_i-r_i, $i \in \{1, 2\}$ pairs and it is re-written as

$$\mathbb{R}_1^{\mathrm{R,N}} = \xi_{r_1} - \left(\frac{\sqrt{\mathbb{P}_U d_{Ur_1}^{-\alpha}}\hbar^{\mathrm{N}}_{Ur_1}}{\sqrt{\mathbb{P}_{t_2} d_{t_2r_1}^{-\alpha}}\hbar^{\mathrm{R}}_{t_2r_1}}\right)\xi_{r_2}. \tag{17}$$

In the derivation of the PDF of TNC, $\mathbb{R}_1^{\mathrm{R,N}}$ is replaced by z, and take the fact that channels do not change during a communication cycle. As a result, these channel coefficients have little effect on the PDF during that communication cycle, and we can replace the channel coefficient ratio with its mean value [8] and write the coefficient of ξ_{r_2} as $\mathcal{A} = \left(\frac{\sqrt{\mathbb{P}_U d_{Ur_1}^{-\alpha}}}{\sqrt{\mathbb{P}_{t_2} d_{t_2r_1}^{-\alpha}}}\mathrm{E}\left[\frac{\hbar^{\mathrm{N}}_{Ur_1}}{\hbar^{\mathrm{R}}_{t_2r_1}}\right]\right)$. Putting $\mathbb{R}_1^{\mathrm{R,N}} = z$ and coefficient of ξ_{r_2} as $\mathcal{A}$ in (17) and re-written (17) as

$$Z = \xi_{r_1} - \mathcal{A}\xi_{r_2}. \tag{18}$$

Here ξ_{r_1} and ξ_{r_2} are the AWGN having mean zero and variance $\sigma^2_{\xi_{r_1}}$ and $\sigma^2_{\xi_{r_2}}$, respectively. The PDF of ξ_{r_1} and ξ_{r_2} are

$$f_{\xi_{r_1}} = \frac{1}{\sqrt{2\pi\sigma^2_{\xi_{r_1}}}}e^{-\frac{\xi^2_{r_1}}{2\sigma^2_{\xi_{r_1}}}},$$
$$f_{\xi_{r_2}} = \frac{1}{\sqrt{2\pi\sigma^2_{\xi_{r_2}}}}e^{-\frac{\xi^2_{r_2}}{2\sigma^2_{\xi_{r_2}}}}. \tag{19}$$

By using transformation on (18), the PDF of TNC is defined as

$$f_Z(z) = \int_0^z f_{\xi_{r_1}}(z + \mathcal{A}p) f_{\xi_{r_2}}(p)dp. \tag{20}$$

After putting $f_{\xi_{r_1}}$ and $f_{\xi_{r_2}}$ from (19) into (20) and integrating them, we obtain the PDF of TNC as follows

$$f_Z(z) = \frac{e^{-\frac{z^2}{2\left(A^2\sigma^2_{\xi_{r_1}}+\sigma^2_{\xi_{r_2}}\right)}}\sqrt{\frac{\pi}{2}}\left(\mathcal{A}_1 - \mathcal{A}_2\right)}{2\pi\sqrt{A^2\sigma^2_{\xi_{r_1}} + \sigma^2_{\xi_{r_2}}}}, \tag{21}$$

where $\mathcal{A}_1$ and $\mathcal{A}_2$ defined in (21) are given as

$$\mathcal{A}_1 = \mathrm{Erf}\left[\frac{Z\left(A(1+A)\sigma^2_{\xi_{r_1}} + \sigma^2_{\xi_{r_2}}\right)}{\sqrt{2}\sigma_{\xi_{r_1}}\sigma_{\xi_{r_2}}\sqrt{A^2\sigma^2_{\xi_{r_1}} + \sigma^2_{\xi_{r_2}}}}\right],$$
$$\mathcal{A}_2 = \mathrm{Erf}\left[\frac{AZ\sigma_{\xi_{r_1}}}{\sqrt{2}\sigma_{\xi_{r_2}}\sqrt{A^2\sigma^2_{\xi_{r_1}} + \sigma^2_{\xi_{r_2}}}}\right], \tag{22}$$

where Erf [.] denotes error function.

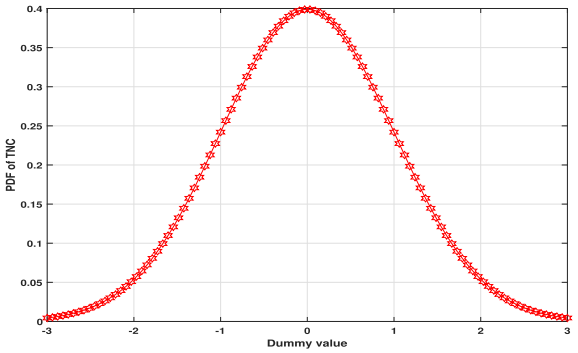

FIGURE 4. PDF of TNC with dummy variable z.

PDF of TNC with some dummy value is shown in Fig. 4. This PDF is useful at the receiver end of the UA-NCC system for extracting the 2nd copy of the desired signal. The network designer can design the receiver circuitry in such a way by taking care of the statistical parameters of TNC, such that the decoding (or calculating bit error rate) of the received packets at the receiver nodes having error free.

IV. DIFFERENT METRICS FOR PERFORMANCE EVALUATION OF UA-NCC SYSTEM

This section derives the expressions of spectral efficiency and throughput along with the closed-form expression of an outage probability for the UA-NCC system in the Nakagami-m fading environment. In order to account for battery limits and the size constraints of tiny devices, we use SC in place of MRC and equal gain combining (EGC) at the r_i node for evaluating the above performance metrics. Furthermore, to achieve a better quality of service, DF is used at UAV in place of the AF relaying scheme in this work.

A. SPECTRAL EFFICIENCY

The spectral efficiency (SE) at the desired receiving node (r_i) is represented by the symbol $\mathbb{I}_{\text{UA-NCC}}$ and is defined as [4].

$$\mathbb{I}_{\text{UA-NCC}}(r_i) = \frac{1}{N+1}\min\{\log_2(1+\Upsilon_{t_iU}), \log_2(1+\max(\Upsilon_{t_ir_i}, \Gamma_{t_iUr_i}))\}, \quad (23)$$

where Υ_{t_ik} represents signal-to-noise ratio (SNR) between trasmitting node t_i and receiving $k \in \{U, r_i\}$, which is defined as

$$\Upsilon_{jk} = \frac{\mathbb{P}_j d_{jk}^{-\alpha}|\hbar_{jk}|^2}{\sigma_k^2}, \quad (24)$$

Symbol $\Upsilon_{t_iUr_i}$ denotes the SNR at r_i, when signal x_i reaches at r_i via U and it is given by

$$\Upsilon_{t_iUr_i} = \frac{\Upsilon_{Ur_i}}{1+\sum_{j=1,j\neq i}^{N}\left(\frac{\Upsilon_{Ur_i}}{\Upsilon_{t_jr_i}}\right)}. \quad (25)$$

SNR used in (25), can be found by using (24). The SE for the UA-NCC system, which includes the SEs for all N receiving nodes (r_i), is calculated by averaging individual SEs and given as follows

$$\eta = \frac{\sum_{i=1}^{N}\mathbb{I}_{\text{UA-NCC}}(r_i)}{N}, \quad (26)$$

where the SEs of each r_i can be calculated by using (23).

Algorithm 1 Proposed Method for Evaluation of Throughput

Input : N, *iteration*, h_D, r_j, pre-defined threshold (t_{th}).
Output: Evaluation of throughput for t_i-r_i pair

1 **for** q=*1*→*iteration* **do**
2 **for** i=*1*→*length*(h_D) **do**
3 Calculate χ_L and χ_{NL} for a given h_D and $d_{Ot_i(r_i)}$.
4 Calculate m for a given h_D and $d_{Ot_i(r_i)}$.
5 Evaluate $\hbar_{t_1U}, \hbar_{t_2U}, \ldots, \hbar_{t_NU}, \hbar_{Ur_i}$ channels based on m
6 Evaluate SE using (23)
7 $\mathcal{O}_1$=$\mathbb{I}_{\text{UA-NCC}}(r_i) > t_{th}$
8 μ_i(q,i)=length(find($\mathcal{O}_1$))
9 **end**
10 **end**
11 Calculate Throughput (μ)=mean(μ_i).

B. THROUGHPUT

It is an important performance metric in wireless communication for measuring the quality of service. Throughput of the UA-NCC system for the desired t_i-r_i pair at a given pre-defined threshold value (t_{th}) can be defined as

$$\mu_i = \frac{\mathcal{Z}_i}{\mathcal{T}}, \quad (27)$$

where $\mathcal{Z}_i$ is the number of bits received successfully at the node r_i and $\mathcal{T}$ is the total time duration for completing one communication cycle. *Algorithm 1* is designed to evaluate the throughput of the UA-NCC system for the proposed scenario. The throughput for the UA-NCC system by including N receiving nodes is calculated as

$$\mu = \frac{\sum_{i=1}^{N}\mu_i}{N} \quad (28)$$

where μ_i denotes the throughput corresponding to each desire t_i-r_i pair. The calculation of throughput in *Algorithm 1* is explained as follows: In step 3, for a given h_D and r_j, we have calculated χ_L and χ_{NL} and then calculated the path loss exponent (using (2)). In step 4, the Nakagami-m shaping parameter is calculated for the same h_D and r_j and then calculate Nakagami-m channels ($\hbar_{t_1U}$, $\hbar_{t_2U}$,..., $\hbar_{t_NU}$ and $\hbar_{Ur_i}$) as mentioned in step 5. Based on the path loss-exponent and shaping parameter calculated in steps 3 and 4, large-scale

path loss and channel gain are evaluated. In steps 6 and 7 evaluate the number of bits received at r_i using the parameters evaluated in steps 3,4, and 5. Finally, we have calculated the throughput at r_i using (28) in step 11.

C. OUTAGE PROBABILITY

Outage probability is another important metric for measuring the performance of UA-NCC system. For a given spectral efficiency $\mathcal{K}$, the outage probability at node r_i is defined as [8] and [40]

$$\mathbb{P}_{\text{out}}(r_i) = \mathbb{P}\left[\mathbb{I}_{\text{UA-NCC}}(r_i) < \mathcal{K}\right]. \tag{29}$$

Using (23) and (29), outage probability for UA-NCC system becomes

$$\mathbb{P}_{\text{out}}(r_i) = \mathbb{P}\Big[\min\{\log_2(1+\Upsilon_{t_iU}), \log_2(1+\max(\Upsilon_{t_ir_i}, \Upsilon_{t_iUr_i}))\} < (N+1)\mathcal{K}\Big]. \tag{30}$$

Using probability theory, (30) can be rewritten in (31), as shown at the bottom of the page, where $T = (2^{(N+1)\mathcal{K}} - 1)$. In (31), 3rd term can be denoted by $\mathbb{P}_{\text{out}}^{\text{3rd}}$ and can be written as

$$\mathbb{P}_{\text{out}}^{\text{3rd}}(r_i) = \underbrace{\mathbb{P}[\Upsilon_{t_ir_i} < T]}_{\text{1st part}} \underbrace{\mathbb{P}[\Upsilon_{t_iUr_i} < T]}_{\text{2nd part}}. \tag{32}$$

To the best of authors knowledge, solution of 2nd part of (32) is not available with the current form of $\Upsilon_{S_iRD_i}$. To obtain a closed-form expression, we used an approximation [41] for $\Upsilon_{t_iUr_i}$ from equation (32) and then reformulated (32) as follows

$$\Upsilon_{t_iUr_i} \approx \bar{\Upsilon}_{t_iUr_i} = \min(\Upsilon_{Ur_i}, \Upsilon_{t_1r_i}, \ldots, \Upsilon_{t_{i-1}r_i}, \Upsilon_{t_{i+1}r_i}, \ldots, \Upsilon_{t_Nr_i}). \tag{33}$$

Using (33) in (32) and solve 2nd part of (32) as below

$$\mathbb{P}[\Upsilon_{t_iUr_i} < T] = 1 - \underbrace{\mathbb{P}[\Upsilon_{Ur_i} > T]}_{\text{3rd part}} \underbrace{\prod_{j=1, j\neq i}^{N} \mathbb{P}[\Upsilon_{t_jr_i} > T]}_{\text{4th part}}. \tag{34}$$

The PDF and the cumulative distribution function (CDF) for Υ_{jk} are given by [2]

$$f_V(v) = \left(\frac{m_v}{\lambda_v}\right)^{m_v} \frac{v^{m_v-1}}{\Gamma(m_v)} \exp\left(-\frac{m_v v}{\lambda_v}\right), \tag{35}$$

and

$$F_V(v) = \frac{1}{\Gamma(m_v)} \gamma\left(m_v, \frac{m_v v}{\lambda_v}\right), \tag{36}$$

where $v \in \{\Upsilon_{t_iU}, \Upsilon_{t_ir_i}, \Upsilon_{t_{j\neq i}U}, \Upsilon_{Ur_i}\}$, m_v is known as shaping parameter of Nakagami-m fading, Γ and γ denote Gamma and lower incomplete Gamma function, respectively and $\lambda_v = \frac{\mathbb{P}_j d_{jk}^{-\alpha} \mathrm{E}[|\hbar_{jk}|^2]}{\sigma_k^2}$. Solution of 1st term of (31) can be obtain as [42]

$$\mathbb{P}[\Upsilon_{t_iU} < T] = \int_0^T \left(\frac{m_v}{\lambda_v}\right)^{m_v} \frac{v^{m_v-1}}{\Gamma(m_v)} \exp\left(-\frac{m_v v}{\lambda_v}\right) dv = \frac{1}{\Gamma(m_{t_iU})} \gamma\left(m_{t_iU}, \frac{m_{t_iU} T}{\lambda_{t_iU}}\right), \tag{37}$$

where $\lambda_{t_iU} = \frac{\mathbb{P}_{t_i} d_{t_iU}^{-\alpha} \mathrm{E}[|\hbar_{t_iU}|^2]}{\sigma_U^2}$. Solution of the 1st part of the 2nd term of (31) can be expressed as

$$\mathbb{P}[\Upsilon_{t_iU} > T] = \int_T^\infty \left(\frac{m_v}{\lambda_v}\right)^{m_v} \frac{v^{m_v-1}}{\Gamma(m_v)} \exp\left(-\frac{m_v v}{\lambda_v}\right) dv = 1 - \frac{1}{\Gamma(m_{t_iU})} \Gamma\left(m_{tiU}, \frac{m_{t_iU} T}{\lambda_{t_iU}}\right). \tag{38}$$

Solution of the 2nd part of the 2nd term of (31) can be obtained as

$$\prod_{j=1, j\neq i}^{N} \mathbb{P}[\Upsilon_{t_jU} > T] = \prod_{j=1, j\neq i}^{N} \left[1 - \frac{1}{\Gamma(m_{t_jU})} \Gamma\left(m_{t_jU}, \frac{m_{t_jU} T}{\lambda_{t_jU}}\right)\right]. \tag{39}$$

Similarly, solution of 1st parts of (32) and solution of 3rd parts of (34) can be written as

$$\mathbb{P}[\Upsilon_{t_ir_i} < T] = [1 - e^{\lambda_{t_ir_i} T}], \tag{40}$$

and

$$\mathbb{P}[\Upsilon_{Ur_i} > T] = 1 - \frac{1}{\Gamma(m_{Ur_i})} \Gamma\left(m_{Ur_i}, \frac{m_{Ur_i} T}{\lambda_{Ur_i}}\right). \tag{41}$$

Solution of 4th part of (34) can be obtained as

$$\prod_{j=1, j\neq i}^{N} \mathbb{P}[\Upsilon_{t_jr_i} > T] = e^{-\left[\sum_{j=1, j\neq i}^{N} \lambda_{t_jr_i} T\right]}. \tag{42}$$

$$\mathbb{P}_{\text{out}}(r_i) = \underbrace{\mathbb{P}[\Upsilon_{t_iU} < T]}_{\text{1st term}} + \underbrace{\Bigg[\underbrace{\mathbb{P}[\Upsilon_{t_iU} > T]}_{\text{1st part}} \underbrace{\prod_{j=1, j\neq i}^{N} \mathbb{P}[\Upsilon_{t_jU} > T]}_{\text{2nd part}}\Bigg]}_{\text{2nd term}} \underbrace{\mathbb{P}[\max(\Upsilon_{t_ir_i}, \Upsilon_{t_iUr_i}) < T]}_{\text{3rd term}}. \tag{31}$$

Invoking (41) and (42) in (34) and rewritten (34) as

$$\mathbb{P}[\Upsilon_{t_iUr_i} < T] = 1 - \left[1 - \frac{1}{\Gamma(m_{Ur_i})}\Gamma\left(m_{Ur_i}, \frac{m_{Ur_i}T}{\lambda_{Ur_i}}\right)\right] e^{-\left[\sum_{j=1,j\neq i}^{N} \lambda_{t_jr_i}T\right]}. \quad (43)$$

Remark: The expression derived in (43) is useful in such a scenarios where the direct link between the desired t_i-r_i pair is not exist or goes in highly deep fading condition. In such scenarios, the desired node (r_i) receives the desired signal via UAV.

Using (40) and (43) in (32), we can obtain $\mathbb{P}_{\text{out}}^{\text{3rd}}$ in (44), as shown at the bottom of the page. Putting (37), (40) and (32) in (31), we can obtain outage probability for Nakagami-m channel model as given in (45), as shown at the bottom of the page. The outage probability for UA-NCC system that include all the N receiving nodes (r_i) is defined as

$$\mathbb{P}_{\text{out}} = \frac{\sum_{i=1}^{N} \mathbb{P}_{\text{out}}(r_i)}{N}. \quad (46)$$

where (45) can be used to find $\mathbb{P}_{\text{out}}$ for each r_i node.

V. RESULTS AND ANALYSIS

In this section, we illustrate the performance of the considered UA-NCC system in Nakagami-m faded environment and compare the results with the existing channel models. The simulation parameters used in this work are as follows: The number of transmitted bits is 1000, the number of nodes is four, the power for each transmitting node is 1 mW, the noise power is 10^{-4} W, and the path-loss exponents for the LoS and NLoS components are α_L=2 and α_{NL}=3.5, respectively. Bandwidth in the network is 100 MHz. The environment parameters are j_1=1, j_2=6. The pre-defined threshold value for comparing the received signal strength is 0.01, the range of vertical heights is 0:50m and the horizontal distance between ground nodes is 100m. Monte-Carlo simulation using MATLAB R2021b has been carried out for validating the analytical results.

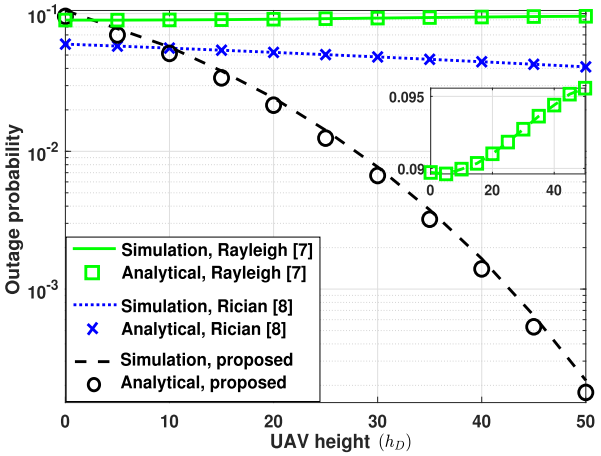

FIGURE 5. Comparision of probability of outage with UAV height [meter] for different channel model.

Fig. 5 shows the probability of outage with UAV height for different channel models. Here, we compare the results by using the three-channel models. The 1st model, the Rayleigh [8] model, assumes that all links within the UA-NCC system exhibit Rayleigh fading. In the 2nd model, the Rician [9] model, the A2G links are characterized as Rician distributed, while the ground nodes are assumed to undergo Rayleigh fading. The 3nd model introduces the proposed Nakagami-m channel model, where the G2A and A2G links are modelled as Nakagami-m distributed. It's worth noting that the parameter m changes depending on the height of the UAV. At the same time, the ground nodes experience Rayleigh fading in this model. At h_D=0, it is observed that the 1st and 3rd models having similar performance due to the same value of m (m=1), resulting in Rayleigh fading. Meanwhile, the 2nd model showcases superior performance compared to the 1st and 3rd models, primarily because its A2G links follow a Rician distribution. The performance of 1st model decreases with UAV height increases, because in this case, path-loss increases with UAV height, similarly the performance of 2nd and 3rd models also increases with the UAV height due to increase in the LoS

$$\mathbb{P}_{\text{out}}^{\text{3rd}} = [1 - e^{-\lambda_{t_ir_i}T}]\left[1 - \left[1 - \frac{1}{\Gamma(m_{Ur_i})}\Gamma\left(m_{Ur_i}, \frac{m_{Ur_i}T}{\lambda_{Ur_i}}\right)\right] e^{-\left[\sum_{j=1,j\neq i}^{N} \lambda_{t_jr_i}T\right]}\right]. \quad (44)$$

$$\mathbb{P}_{\text{out}}(r_i) = \left[\frac{1}{\Gamma(m_{t_iU})}\gamma\left(m_{t_iU}, \frac{m_{t_iU}T}{\lambda_{t_iU}}\right)\right] + \left[1 - \frac{1}{\Gamma(m_{t_iU})}\Gamma\left(m_{t_iU}, \frac{m_{t_iU}T}{\lambda_{t_iU}}\right)\right] \left[\prod_{j=1,j\neq i}^{N}\left[1 - \frac{1}{\Gamma(m_{t_jU})}\Gamma\left(m_{t_jU}\frac{m_{t_jU}T}{\lambda_{t_jU}}\right)\right]\right] \left[1 - e^{-\lambda_{t_ir_i}T}\right]\left[1 - \left[1 - \frac{1}{\Gamma(m_{Ur_i})}\Gamma\left(m_{Ur_i}, \frac{m_{Ur_i}T}{\lambda_{Ur_i}}\right)\right]\left[e^{-\left[\sum_{j=1,j\neq i}^{N} \lambda_{t_jr_i}T\right]}\right]\right]. \quad (45)$$

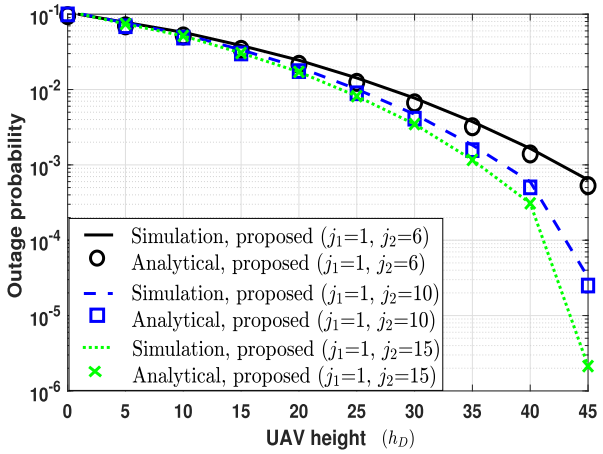

FIGURE 6. Comparision of probability of outage with UAV height [meter] for different environmental parameters.

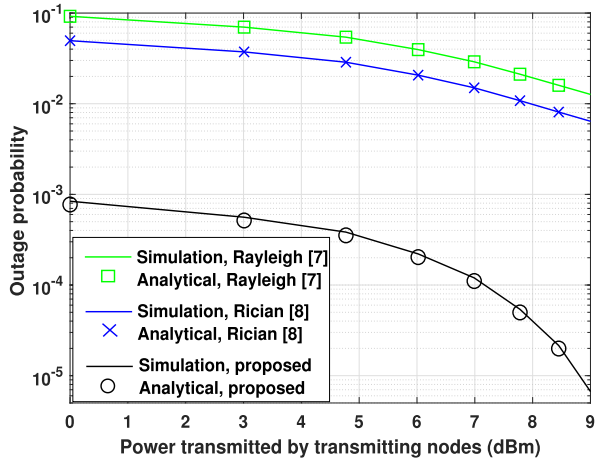

FIGURE 7. Comparison of probability of outage with power transmitted by nodes for different channel model.

component. Here, it is also to be noted that the performance of 2nd model is better up to $h_D \approx$10m compared to the 1st and 3rd channel models. This is attributed to the dominance of the Rician factor over m within this UAV height. The outage performance of the 2nd model and the 3rd model is equivalent at h_D=10m due to the similar value of m and the Rician factor (K), where this relation is defined as $m = \frac{(K+1)^2}{2K+1}$. The performance of the proposed model (3rd model) is better beyond 10m as compared to the existing Rician channel model because of the higher value of m over K.

Fig. 6 shows the outage probability with UAV height of our proposed (Nakagami-m) model for different environmental parameters. Here, we compare the results for different values of j_2 for fixed value of j_1. As observed from (1), the channel gain of Nakagami-m fading channel model increases with increase in the value of j_2, thereby improving the overall outage performance of UA-NCC system.

Fig. 7 shows the variation of the outage probability with power transmitted by the transmitting nodes in the different channel models when the UAV is placed at a height of 50m.

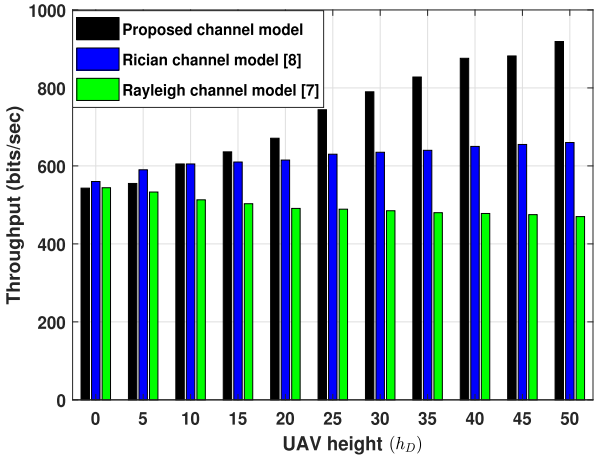

FIGURE 8. Comparison of throughput with UAV height [meter] for different channel model.

It is worth noting here that if the desired user wants the outage probability to be less than 10^{-3} over the entire range of transmitting power as shown on the horizontal axis, the user can meet that requirement by using the proposed channel (Nakagami-m) model rather than the existing Rayleigh and Rician channel models. This gives useful insight to the network designer for choosing the channel for G2A and A2G links in the UA-NCC system, which is helpful in practical applications such as disaster management etc.

Fig. 8 shows the variation of throughput with UAV height in the different channel models. Here, it may be noted that the number of bits received at the desired destination decreases as the UAV height increases in the case of a Rayleigh fading channel. This may happen because in a Rayleigh fading channel there is no LoS component, only a NLoS component exists. Therefore, the channel gain decreases and large-scale path-loss increases with UAV height. While in the case of Rician and the proposed channel (Nakagami-m) model, the number of bits received at the destination node increases with UAV height. It may happen because the LoS component increases with the UAV height, which is dominated by the large-scale path-loss. Another observation is that the received bits in the proposed channel model are greater than that of in the Rician channel model, because the value of the shaping parameter (m) is much higher beyond 10m than the Rician factor (K).

Fig. 9 shows the variation of the outage probability with rate in the different channel models. It may be noted here that for a given required rate at the destination node, the performance of the proposed channel (Nakagami-m) model is better as compared to the existing Rayleigh and Rician channel models.

This also gives insightful information to the system engineer to design the receiver circuitry, to choose G2A and A2G links in favor of the proposed channel (Nakagami-m) model in place of the existing Rayleigh and Rician channel models for a given pair of outages and rates (let's say $\mathbb{P}_{\text{out}}$=10^{-4}, required rate=0.23).

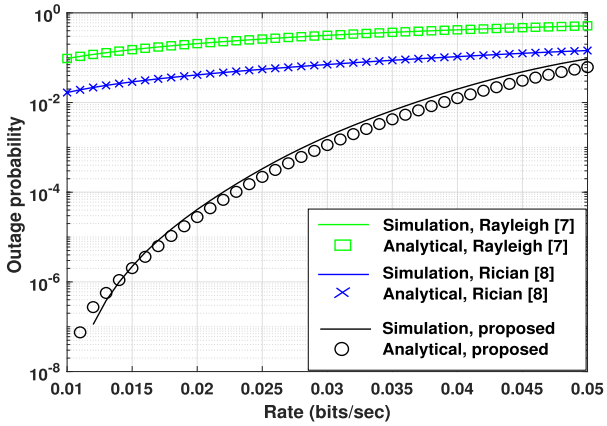

FIGURE 9. Comparison of probability of outage with rate [bits/sec] for different channel model.

VI. CONCLUSION

In this paper, the height-dependent Nakagami-*m* shaping parameter and height-dependent path-loss model are proposed for analyzing the performance of UAV-assisted network-coded cooperation (UA-NCC) system. The analytical framework for the UA-NCC system using the proposed Nakagami-*m* channel has been developed. For evaluating the performance of the UA-NCC system, we have developed the expressions of spectral efficiency and throughput. The closed-form expression of the outage probability is derived for the UA-NCC system. The statistical parameters such as mean, variance, and probability density function (PDF) of the total noise component (TNC) are analyzed for the proposed system model to achieve error-free communication. An extensive simulation has been carried out to verify the analytical analysis. The results show that the UA-NCC system's performance in the Nakagami-*m* fading channel is more realistic than the existing Rayleigh and Rician faded channels. The proposed work is useful in the area of internet of things (IoT)-based smart agriculture. Energy harvesting at the UAV for the proposed work is also an intriguing future project.

REFERENCES

[1] G. Yao, H. Chen, and J. Hu, "An improved expectation propagation based detection scheme for MIMO systems," *IEEE Trans. Commun.*, vol. 69, no. 4, pp. 2163–2175, Apr. 2021.

[2] T. M. Hoang, B. C. Nguyen, P. T. Tran, and L. T. Dung, "Outage analysis of RF energy harvesting cooperative communication systems over Nakagami-*m* fading channels with integer and non-integer *m*," *IEEE Trans. Veh. Technol.*, vol. 69, no. 3, pp. 2785–2801, Mar. 2020.

[3] X. Liu, X. Gong, and Y. Zheng, "Reliable cooperative communications based on random network coding in multi-hop relay WSNs," *IEEE Sensors J.*, vol. 14, no. 8, pp. 2514–2523, Aug. 2014.

[4] S. Sharma, Y. Shi, J. Liu, Y. T. Hou, S. Kompella, and S. F. Midkiff, "Network coding in cooperative communications: Friend or foe?" *IEEE Trans. Mobile Comput.*, vol. 11, no. 7, pp. 1073–1085, Jul. 2012.

[5] S. Bhattacharyya, P. Kumar, S. Darshi, O. Burnwal, and K. Singhal, "Full duplex relay assisted coded cooperation for next generation wireless networks," in *Proc. IEEE 18th India Council Int. Conf. (INDICON)*, Dec. 2021, pp. 1–6.

[6] S. Bhattacharyya, P. Kumar, S. Darshi, S. Agarwal, and S. Shailendra, "Cross layer MAC protocol for a peer conscious opportunistic network coded cooperation system," *IEEE Trans. Mobile Comput.*, vol. 22, no. 12, pp. 7014–7026, Dec. 2023.

[7] S. Bhattacharyya, P. Kumar, S. Darshi, S. Majhi, B. Kumbhani, and A. A. Almohammedi, "Hybrid relaying based cross layer MAC protocol using variable beacon for cooperative vehicles," *IEEE Trans. Veh. Technol.*, vol. 73, no. 1, pp. 258–267, Jan. 2024.

[8] P. Kumar, P. Singh, S. Darshi, and S. Shailendra, "Analysis of drone assisted network coded cooperation for next generation wireless network," *IEEE Trans. Mobile Comput.*, vol. 20, no. 1, pp. 93–103, Jan. 2021.

[9] P. Kumar, S. Bhattacharyya, S. Darshi, A. Sharma, A. A. Almohammedi, V. Shepelev, and S. Shailendra, "Drone assisted network coded cooperation with energy harvesting: Strengthening the lifespan of the wireless networks," *IEEE Access*, vol. 10, pp. 43055–43070, 2022.

[10] P. Kumar, S. Bhattacharyya, S. Darshi, S. Majhi, A. A. Almohammedi, and S. Shailendra, "Outage analysis using probabilistic channel model for drone assisted multi-user coded cooperation system," *IEEE Trans. Veh. Technol.*, vol. 72, no. 8, pp. 10273–10285, Aug. 2023.

[11] A. Kumar, S. Majhi, and H.-C. Wu, "Physical-layer security of underlay MIMO-D2D communications by null steering method over Nakagami-*m* and Norton fading channels," *IEEE Trans. Wireless Commun.*, vol. 21, no. 11, pp. 9700–9711, Nov. 2022.

[12] B. Ji, Y. Li, S. Chen, C. Han, C. Li, and H. Wen, "Secrecy outage analysis of UAV assisted relay and antenna selection for cognitive network under Nakagami-*m* channel," *IEEE Trans. Cognit. Commun. Netw.*, vol. 6, no. 3, pp. 904–914, Sep. 2020.

[13] M. Monemi and H. Tabassum, "Performance of UAV-assisted D2D networks in the finite block-length regime," *IEEE Trans. Commun.*, vol. 68, no. 11, pp. 7270–7285, Nov. 2020.

[14] S. K. Singh, K. Agrawal, K. Singh, and C.-P. Li, "Outage probability and throughput analysis of UAV-assisted rate-splitting multiple access," *IEEE Wireless Commun. Lett.*, vol. 10, no. 11, pp. 2528–2532, Nov. 2021.

[15] X. Pang, M. Liu, N. Zhao, Y. Chen, Y. Li, and F. R. Yu, "Secrecy analysis of UAV-based mmWave relaying networks," *IEEE Trans. Wireless Commun.*, vol. 20, no. 8, pp. 4990–5002, Aug. 2021.

[16] Z. Wang and J. Zheng, "Rate meta distribution of downlink base station cooperation for cellular-connected UAV networks," *IEEE Commun. Lett.*, vol. 27, no. 2, pp. 756–760, Feb. 2023.

[17] R. R. Yakkati, R. R. Yakkati, R. K. Tripathy, and L. R. Cenkeramaddi, "Radio frequency spectrum sensing by automatic modulation classification in cognitive radio system using multiscale deep CNN," *IEEE Sensors J.*, vol. 22, no. 1, pp. 926–938, Jan. 2022.

[18] A. Y. Al-Zahrani, "Optimal 3-D placement of an aerial base station in a heterogeneous wireless IoT with Nakagami-*m* fading channels," *Ad Hoc Sens. Wireless Netw.*, vol. 46, nos. 3–4, pp. 309–328, 2020.

[19] N. L. Prasad and B. Ramkumar, "3-D deployment and trajectory planning for relay based UAV assisted cooperative communication for emergency scenarios using Dijkstra's algorithm," *IEEE Trans. Veh. Technol.*, vol. 72, no. 4, pp. 5049–5063, Apr. 2023.

[20] W. Wang, X. Li, R. Wang, K. Cumanan, W. Feng, Z. Ding, and O. A. Dobre, "Robust 3D-trajectory and time switching optimization for dual-UAV-enabled secure communications," *IEEE J. Sel. Areas Commun.*, vol. 39, no. 11, pp. 3334–3347, Nov. 2021.

[21] H. Li, J. Li, M. Liu, and F. Gong, "UAV-assisted secure communication for coordinated satellite-terrestrial networks," *IEEE Commun. Lett.*, vol. 27, no. 7, pp. 1709–1713, Jul. 2023.

[22] S. K. Singh, K. Agrawal, K. Singh, C.-P. Li, and W.-J. Huang, "On UAV selection and position-based throughput maximization in multi-UAV relaying networks," *IEEE Access*, vol. 8, pp. 144039–144050, 2020.

[23] R. Bajpai, H. Ramesh, N. Gupta, and V. A. Bohara, "Outage analysis of multicarrier full-duplex cooperative UAV-to-UAV communications system," *IEEE Wireless Commun. Lett.*, vol. 12, no. 8, pp. 1309–1313, Aug. 2023.

[24] Y. Su, M. Liwang, Z. Chen, and X. Du, "Toward optimal deployment of UAV relays in UAV-assisted Internet of Vehicles," *IEEE Trans. Veh. Technol.*, vol. 72, no. 10, pp. 13392–13405, Oct. 2023.

[25] R. Ma, W. Yang, Y. Zhang, J. Liu, and H. Shi, "Secure mmWave communication using UAV-enabled relay and cooperative jammer," *IEEE Access*, vol. 7, pp. 119729–119741, 2019.

[26] Y. Chen, W. Feng, and G. Zheng, "Optimum placement of UAV as relays," *IEEE Commun. Lett.*, vol. 22, no. 2, pp. 248–251, Feb. 2018.

[27] P. Kumar, S. Darshi, and S. Shailendra, "Analysis of drone assisted network coded cooperation for LoS environments," *Wireless Pers. Commun.*, vol. 127, no. 4, pp. 3493–3510, Dec. 2022.

[28] P. Kumar, S. Bhattacharyya, and S. Darshi, "Outage analysis for drone assisted multi-user coded cooperation," in *Proc. IEEE 18th India Council Int. Conf. (INDICON)*, Dec. 2021, pp. 1–6.

[29] P. Kumar, P. Singh, S. Darshi, and S. Shailendra, "Drone assisted network coded co-operation," in *Proc. IEEE Region 10th Conf. (TENCON)*, Oct. 2019, pp. 1174–1179.

[30] L. Yang, F. Meng, J. Zhang, M. O. Hasna, and M. D. Renzo, "On the performance of RIS-assisted dual-hop UAV communication systems," *IEEE Trans. Veh. Technol.*, vol. 69, no. 9, pp. 10385–10390, Sep. 2020.

[31] M. Hua, L. Yang, Q. Wu, C. Pan, C. Li, and A. L. Swindlehurst, "UAV-assisted intelligent reflecting surface symbiotic radio system," *IEEE Trans. Wireless Commun.*, vol. 20, no. 9, pp. 5769–5785, Sep. 2021.

[32] Z. Liu, S. Zhao, Q. Wu, Y. Yang, and X. Guan, "Joint trajectory design and resource allocation for IRS-assisted UAV communications with wireless energy harvesting," *IEEE Commun. Lett.*, vol. 26, no. 2, pp. 404–408, Feb. 2022.

[33] X. Mu, Y. Liu, L. Guo, J. Lin, and H. V. Poor, "Intelligent reflecting surface enhanced multi-UAV NOMA networks," *IEEE J. Sel. Areas Commun.*, vol. 39, no. 10, pp. 3051–3066, Oct. 2021.

[34] N. Goel and V. Gupta, "Outage analysis of drone assisted cooperative communications for hybrid fading channels," *Wireless Pers. Commun.*, vol. 124, no. 4, pp. 2873–2892, Jun. 2022.

[35] N. Goel and V. Gupta, "Performance analysis of drone assisted cooperative communication in hybrid channel environment," in *Proc. IEEE Int. Conf. Adv. Netw. Telecommun. Syst. (ANTS)*, Dec. 2019, pp. 1–5.

[36] P. Kumar, S. Darshi, and S. Shailendra, "Drone assisted device to device cooperative communication for critical environments," *IET Commun.*, vol. 15, no. 7, pp. 957–972, Apr. 2021.

[37] A. A. Khuwaja, Y. Chen, and G. Zheng, "Effect of user mobility and channel fading on the outage performance of UAV communications," *IEEE Wireless Commun. Lett.*, vol. 9, no. 3, pp. 367–370, Mar. 2020.

[38] Q. Wang, X. Li, S. Bhatia, Y. Liu, L. T. Alex, S. A. Khowaja, and V. G. Menon, "UAV-enabled non-orthogonal multiple access networks for ground-air-ground communications," *IEEE Trans. Green Commun. Netw.*, vol. 6, no. 3, pp. 1340–1354, Sep. 2022.

[39] M. T. Mamaghani and Y. Hong, "On the performance of low-altitude UAV-enabled secure AF relaying with cooperative jamming and SWIPT," *IEEE Access*, vol. 7, pp. 153060–153073, 2019.

[40] P. Kumar, S. Majhi, and Y. Nasser, "Analysis of outage performance of opportunistic AF OFDM relaying in Nakagami-*m* channels," in *Proc. Int. Conf. Adv. Comput., Commun. Informat. (ICACCI)*, Sep. 2016, pp. 2527–2531.

[41] B. Zhang, J. Hu, Y. Huang, M. El-Hajjar, and L. Hanzo, "Outage analysis of superposition-modulation-aided network-coded cooperation in the presence of network coding noise," *IEEE Trans. Veh. Technol.*, vol. 64, no. 2, pp. 493–501, Feb. 2015.

[42] M. M. Azari, F. Rosas, K.-C. Chen, and S. Pollin, "Ultra reliable UAV communication using altitude and cooperation diversity," *IEEE Trans. Commun.*, vol. 66, no. 1, pp. 330–344, Jan. 2018.

PANKAJ KUMAR received the B.Tech. degree (Hons.) in electronics and communication engineering and the M.Tech. degree (Hons.) in digital communication from Dr. A. P. J. Abdul Kalam Technical University, formerly Uttar Pradesh Technical University, Lucknow, India, and the Ph.D. degree from the Indian Institute of Technology Ropar, India. He is currently working as an Assistant Professor with the Department of Information and Communication Technology, Manipal Institute of Technology, Manipal Academy of Higher Education, Manipal, India. His research interests include drone assisted cooperative networks, network coding, network coded cooperation, correlation, D2D communication, energy harvesting, intelligent reflecting surface, and NOMA.

SUDHAN MAJHI (Senior Member, IEEE) received the M.Tech. degree in computer science and data processing from the Indian Institute of Technology Kharagpur, Kharagpur, India, in 2004, and the Ph.D. degree from Nanyang Technological University (NTU), Singapore, in 2008. He was a Postdoctoral Researcher with the University of Michigan–Dearborn, Dearborn, MI, USA; the Institute of Electronics and Telecommunications, Rennes, France; and NTU. He is currently an Associate Professor with the Department of Electrical Communication Engineering, Indian Institute of Science, Bengaluru, India. His research interest includes signal processing for wireless communication.